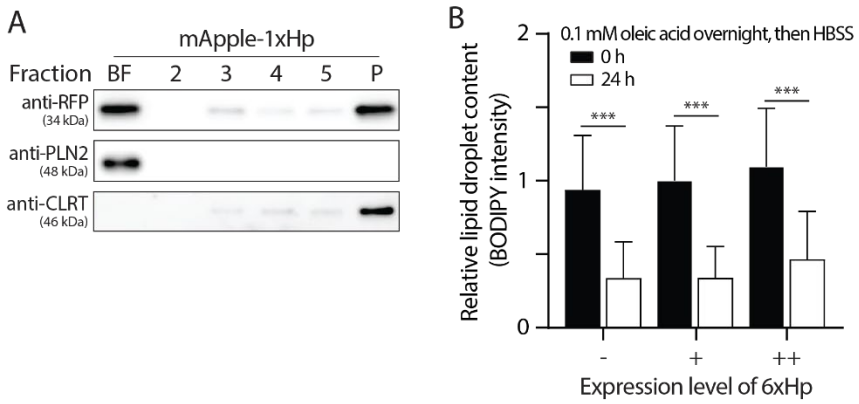

Figure S1. Validation of a synthetic lipid droplet targeting motif.
(A) Distribution of overexpressed mApple-1xHp, endogenous perilipin 2 (PLIN2), and endogenous calreticulin (CLRT) in sucrose-gradient cellular fractionations from HepG2 cells treated with 200 µM oleic acid (OA) overnight. BF, buoyant fraction; P, pellet.
(B) Relative lipid droplet content in OA-loaded, Halo-6xHp overexpressing HeLa cells incubated with HBSS for 0 or 24 h. Mean ± standard deviation are shown (215-1275 cells from two independent experiments). '-' indicates absence of 6xHp expression. + and ++ indicate low and moderate expression of 6xHp, respectively.

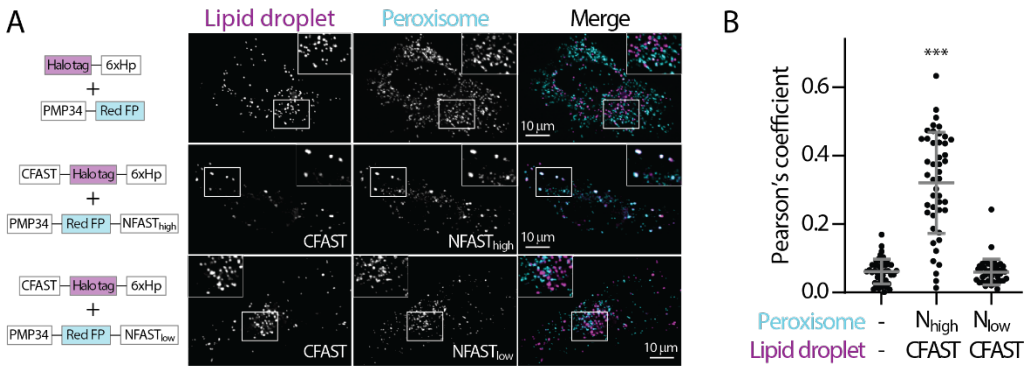

Figure S2. Low affinity splitFAST minimally affects the distribution of lipid droplets and peroxisomes.

(A) Distribution of lipid droplet and peroxisome in oleic acid (OA)-treated HeLa cells overexpressing Halo-6xHp and PMP34-mApple (top), CFAST-Halo-6xHp and PMP34-mApple-$NFAST_{high}$ (middle), or CFAST-Halo-6xHp and PMP34-mApple-$NFAST_{low}$ (bottom) monitored by confocal microscopy. Maximal intensity projected images from six axial slices (1.8 μm in total thickness) are shown.

(B) Quantification of the Pearson's colocalization coefficient of lipid droplet and peroxisome described in (A). Raw data and mean ± standard deviation are shown (44-51 cells from three independent experiments).

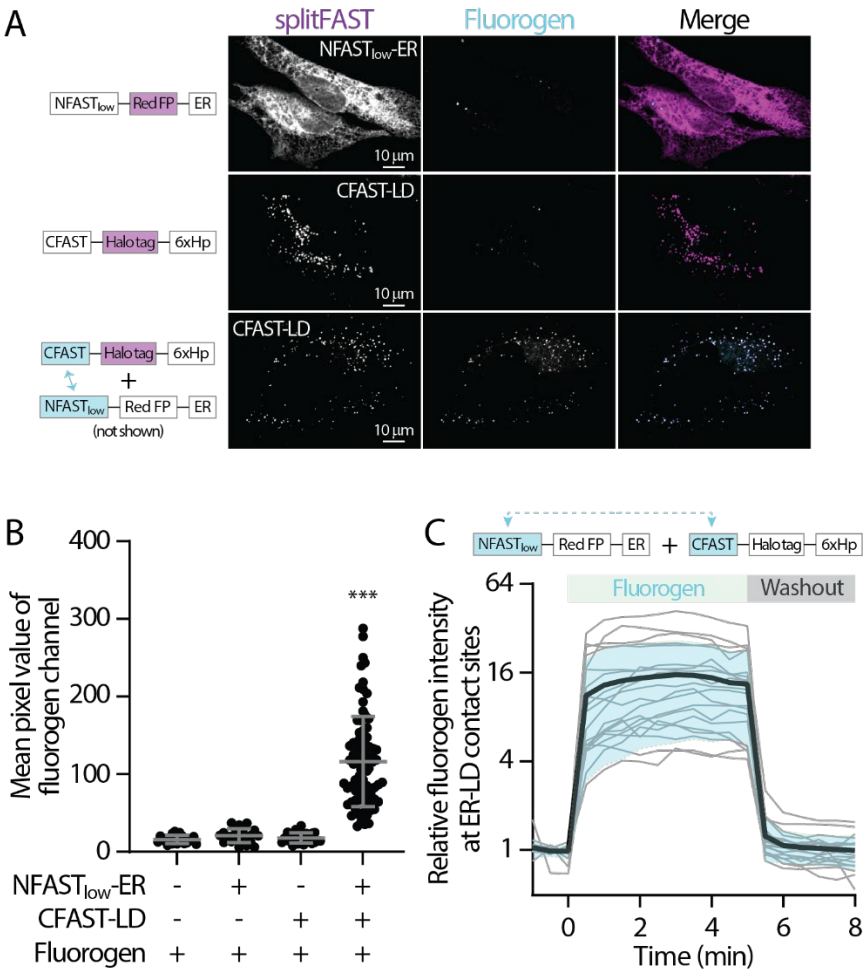

Figure S3. splitFAST remains reversible at organelle contact sites without detectable fluorescence leakiness.

(A) Confocal images of HeLa cells expressing NFAST$_{low}$-mApple-ER (top), CFAST-Halo-6xHp (middle), and NFAST$_{low}$-mApple-ER plus CFAST-Halo-6xHp (bottom) in the presence of HBR-2,5DOM.

(B) Quantification of fluorogen intensity of (A) and in control HeLa cells. Raw data and mean ± standard deviation are shown (22-82 cells).

(C) Relative fluorogen intensity in HeLa cells coexpressing NFAST$_{low}$-mApple-ER and CFAST-Halo-6xHp following HBR-2,5DOM addition and washout monitored by confocal microscopy. Raw data (gray traces) and mean (bold black trace) ± standard deviation (shaded blue) are shown (19-20 cells).

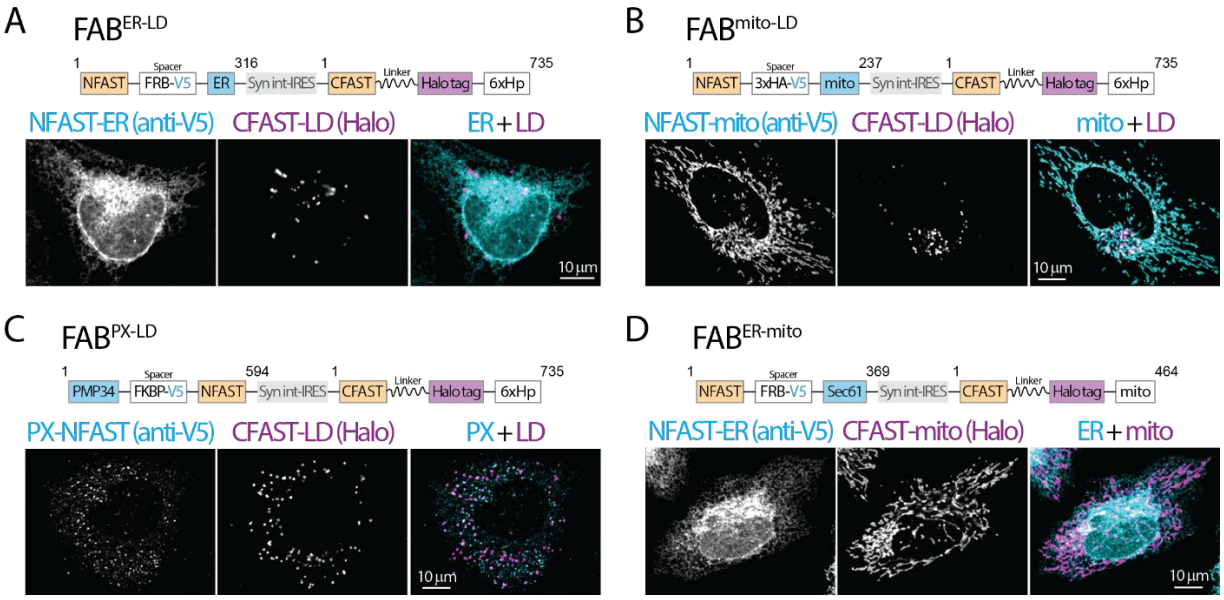

Figure S4. Diagram and validation of FABCON lentiviruses.

(A-D) Diagram (top) and organelle distribution of cognate FABCON halves (bottom) of FAB$^{ER\text{-}LD}$ (A), FAB$^{mito\text{-}LD}$ (B), FAB$^{PX\text{-}LD}$ (C), and FAB$^{ER\text{-}mito}$ (D) monitor by confocal microscope. NFAST fused organelle marker are immunostained with anti-V5 antibody. Maximal intensity projected images from three axial slices (~1 μm in total thickness) are shown. Numbers of amino acids are indicated. Syn int-IRES, synthetic intron-internal ribosome entry site.

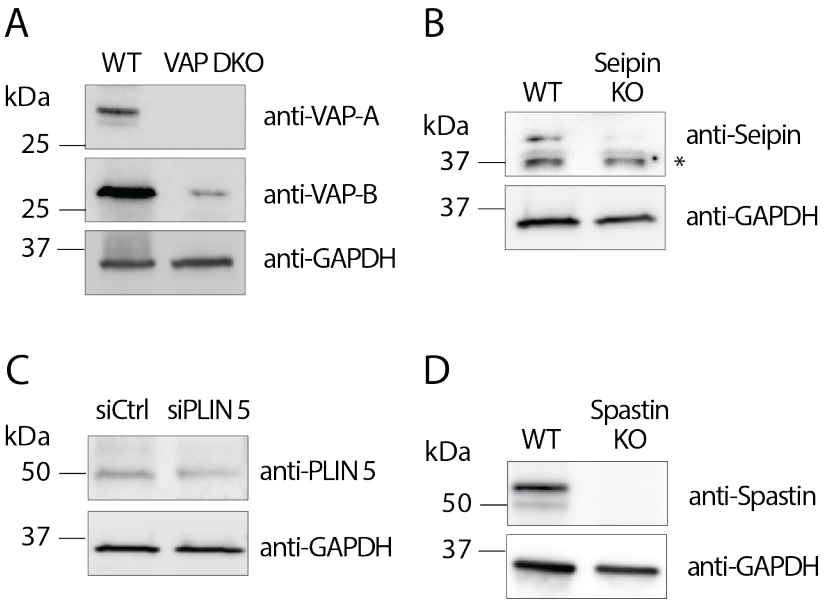

Figure S5. Validation of cell lines via Western blotting.
Endogenous protein levels of VAP-A and VAP-B (A), Seipin (B), PLIN5 (C), and Spastin (D) detected by Western blotting. GAPDH protein levels serve as a loading control. * indicates a non-specific band.

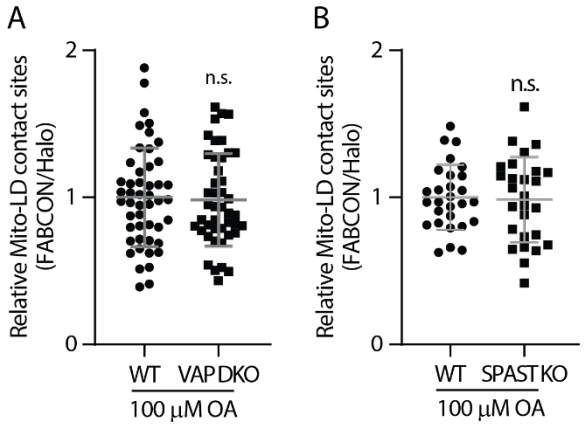

Figure S6. Mito-LD contact sites in VAP DKO and SPAST KO cells.
(A) Relative levels of mito-LD contact sites in oleic (OA)-treated WT and VAP DKO HeLa cells. Raw data and mean ± standard deviation are shown (44-48 cells from two independent experiments).
(B) Relative levels of mito-LD contact sites in OA-treated WT and SPAST KO U2OS cells. Raw data and mean ± standard deviation are shown (27-28 cells from two independent experiments).

Table S1. Organelle targeting motifs.

Organelle	Targeting motif	Validation	Reference
Lipid droplet	6xHp	BODIPY; PLIN2; APEX2	Shown here
ER	Rat Cytochrome b5 TM	Calreticulin	(Cho et al., 2020)
	Sec61β	N/A	N/A
Mitochondria	Human SYNJ2BP TM	Tomm20	(Benedetti et al., 2020)
Peroxisome	Human full-length PMP34	Catalase; PMP70	Shown here

Table S2. Oligonucleotides used in this study.

Name	Sequence (5'-3')
1xHp F (EcoRI)	atcggaattctgagtcgccgcataagcgga
1xHp R (BamHI)	atcgggatccttagctcctcttggctgccatg
PMP34 F (NheI)	atcggctagccaccatggcttccgtgctgtccta
PMP34 R (AgeI)	atcgaccggtaggtgttggtgtgcacgcttca
$NFAST_{high}$ F (NheI)	atcggctagccaccatggagcatgttgcctttgg
$NFAST_{high}$ R (AgeI)	atcgaccggtagagatccccctccgccgctgccgcctcctccgga
$NFAST_{low}$ F (NheI)	atcggctagccaccatggagaccgtgagattcg
$NFAST_{low}$ R (AgeI)	atcgaccggtagagatccccctccgccgctgccgcctcctccggaggtcatggccttcttcatg
$NFAST_{low}$ F (Kpn2I)	atctcaaagcaggtctccg
$NFAST_{low}$ R (NotI)	atcggcggccgcttaggtcatggccttcttcat
IRES N F (NheI)	gaaccgtcagatccgctag
IRES N-ER R (NotI)	atcggcggccgcttagtcctcggccatgtacagg
IRES N-mito R (NotI)	atcggcggccgcttatcaaagttgttgccggtatct
IRES C-LD F (SgsI)	atcgggcgcgccatgggtgacagctattgggtcttt
IRES C-LD R (Acc65I)	atcgggtaccgatccggtggatccttag
Lenti F (InFusion)	ccgtacggaaccggtcgatatctgcggcctagcta
Lenti R (InFusion)	gtacctagtgcggccgccttgtaccgatccggtggat
APEX2 F (NheI)	atcggctagccaccatgggaaagtcttacccaactgt
APEX2 R (EcoRI)	atcggaattccctccggcagagccacctgcactgcctccagctgaggcatcagcaaacccaagc